J. Fluid Mech. (1996), *vol.* 311, *pp.* 343–359

Multiple-timescale analysis of Taylor dispersion in converging and diverging flows

By MICHELLE D. BRYDEN AND HOWARD BRENNER

Department of Chemical Engineering, Massachusetts Institute of Technology, Cambridge, MA 02139-4307, USA

(Received 21 February 1995 and in revised form 13 November 1995)

A multiple-timescale analysis is employed to analyse Taylor-dispersion-like convective–diffusive processes in converging and diverging flows. A long-time asymptotic equation governing the cross-sectionally averaged solute probability density is derived. The form of this equation is shown to be dependent upon the number of spatial dimensions characterizing the duct or 'cone'. The two-dimensional case (non-parallel plates) is shown to be fundamentally different from that for three dimensions (circular cone) in that, in two dimensions, a Taylor dispersion description of the process is possible only for small Péclet numbers or angles of divergence. In contrast, in three dimensions, a Taylor dispersion description is always possible provided sufficient time has passed since the initial introduction of solute into the system. The convective Taylor dispersion coefficients $\overline{D}_c$ for the respective cases of low-Reynolds-number flow between non-parallel plates and in a circular cone are computed and their limiting values, $\overline{D}_c^0$, for zero apex angle are shown to be consistent with the known results for Taylor dispersion between parallel plates and in a circular cylinder. When plotted in the non-dimensional form of $\overline{D}_c/\overline{D}_c^0$ versus the half-vertex angle θ_0, the respective dispersivity results for the two cases hardly differ from one another, increasing monotonically from 1.0 for $\theta_0 = 0$ to approximately 2.6 for a fully flared duct, $\theta_0 = \pi/2$. Lastly, the techniques developed above for the case of rectilinear channel and duct boundaries are extended to the case of curvilinear boundaries, and an illustrative calculation performed for the case of axisymmetric flow in a flared Venturi tube.

1. Introduction

The problem of convective dispersion in ducts of constant cross-section, such as cylinders and parallel plates, has been well-studied. In those studies, the velocity profile and molecular dispersivity are taken to be independent of the axial (global) coordinate. In fact, application of the general theory of macrotransport processes in its current form (Brenner & Edwards 1993) explicitly requires that the phenomenological coefficients appearing in the microscale description of the process be independent of the global-space position. This is closely related to Taylor's (1921) original observation that Taylor dispersion is applicable in circumstances where the axial velocity is a stationary random function of time.

A limited number of studies exist which address problems involving axially varying velocity fields. Thus, Frankel & Brenner (1991) studied Taylor dispersion in unbounded shear flows, allowing the velocity to depend linearly on the global coordinate. Mercer & Roberts (1990) used centre manifold theory to treat the case of dispersion in channels with slowly varying cross-section and thus, varying velocity.

Gill & Güceri (1971) conducted numerical studies of Taylor dispersion in flow between non-parallel flat plates, in addition to having derived a theoretical expression for the axial dispersion coefficient in channels possessing small angles of divergence. Lastly, Smith (1983) derived a expression for the dispersion coefficient in a varying channel whose small depth relative to its width allowed it to be treated as well-mixed in the vertical direction.

The method of multiple-timescales has been used to analyse Taylor dispersion in rectangular ducts (Pagitsas, Nadim & Brenner 1986). This method takes advantage of the separation of timescales required for a macrotransport description of the process to exist. The present contribution presents a multiple-timescale analysis of dispersion between non-parallel flat plates and in a circular cone. The functional dependence of the macrotransport equation upon the dimensionality of the channel is established and circumstances quantified whereby such a dispersion description of the process is indeed possible. The Taylor dispersion coefficients for low-Reynolds-number flow between non-parallel flat plates and in a circular cone are calculated. Finally, an extension of the current multiple-timescale methods to cross-sectionally varying flows in curvilinear channels and ducts is presented, and illustrated by example.

2. Kinematics of flow in an n-dimensional cone

The vector velocity field for axisymmetric radial flow in an n-dimensional cone of apex angle $2\theta_0$ (see figures 1*a* and 1*b*) is of the form

$$\boldsymbol{v} = \boldsymbol{i}_r v_r(r,\theta) \qquad \begin{pmatrix} 0 < r < \infty, & -\theta_0 \leqslant \theta \leqslant \theta_0 \leqslant \pi & (n=2) \\ 0 < r < \infty, & 0 \leqslant \theta \leqslant \theta_0 \leqslant \pi & (n=3) \end{pmatrix}, \tag{2.1}$$

with

$$v_r = \frac{Q(\theta)}{r^{n-1}}. \tag{2.2}$$

Here, the inverse r^{n-1} dependence results from the requirement that the axisymmetric flow field satisfy the continuity equation

$$\frac{1}{r^{n-1}}\frac{\partial}{\partial r}(r^{n-1}v_r) = 0 \tag{2.3}$$

for incompressible radial flow. The algebraically-signed 'volumetric' flow rate through the duct, namely $Q = \int v_r \mathrm{d}S$ (with $\mathrm{d}S$ a scalar element of surface area on the surface $r =$ constant) is given explicitly by the expression

$$Q = 2\pi^{n-2}\int_0^{\theta_0} Q(\theta)\sin^{n-2}\theta \mathrm{d}\theta. \tag{2.4}$$

The exact solution of the Navier–Stokes equations for incompressible Jeffrey–Hamel flow between non-parallel flat plates ($n = 2$) is well known (Rouse 1959; Goldstein 1965*a*) and can be expressed in terms of elliptic functions. For low-Reynolds-number flow this velocity field is

$$v_r = \frac{Q}{r}\frac{\cos 2\theta - \cos 2\theta_0}{\sin 2\theta_0 - 2\theta_0\cos\theta_0} \qquad (n=2). \tag{2.5}$$

While no comparable exact Navier–Stokes solution exists for flow in a circular cone ($n = 3$) (Ackerberg 1965; Goldstein 1965*b*), the velocity field for low-Reynolds-

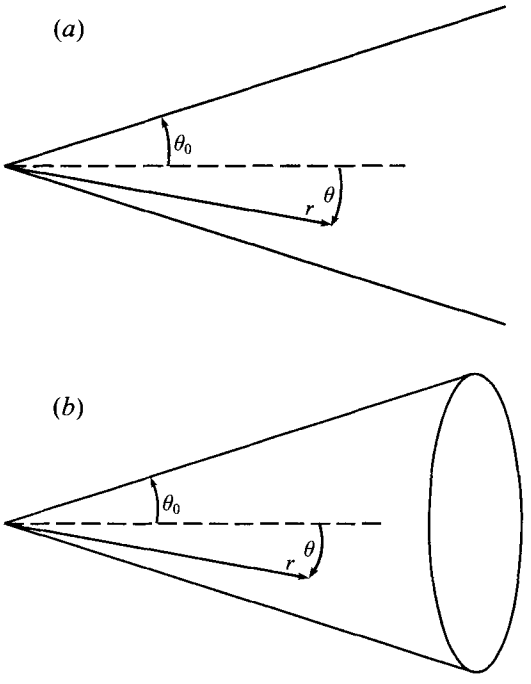

FIGURE 1. (*a*) Non-parallel plates; (*b*) circular cone.

number is (cf. Happel & Brenner 1983)

$$v_r = \frac{3Q}{2\pi r^2}\frac{\cos^2\theta - \cos^2\theta_0}{(1+2\cos\theta_0)(1-\cos\theta_0)^2} \qquad (n=3). \tag{2.6}$$

3. Microscale transport equation for convection and molecular diffusion in a diverging or converging duct

The governing equation for unsteady convection and diffusion of a dissolved or colloidal Brownian species between non-parallel plates or in a circular cone is

$$\frac{\partial C}{\partial t} + \frac{Q(\theta)}{r^{n-1}}\frac{\partial C}{\partial r} + \frac{D}{r^2}\left[\frac{1}{r^{n-3}}\frac{\partial}{\partial r}\left(r^{n-1}\frac{\partial C}{\partial r}\right) - \frac{1}{\sin^{n-2}\theta}\frac{\partial}{\partial\theta}\left(\sin^{n-2}\theta\frac{\partial C}{\partial\theta}\right) - \frac{\delta_{n3}}{\sin\theta}\frac{\partial^2 C}{\partial\phi^2}\right] = 0, \tag{3.1}$$

with D the molecular diffusivity, assumed constant, and δ_{n3} the Kronecker delta. This equation is to be solved for the solute concentration $C(r,\theta,(\phi),t)$ subject to the initial and boundary conditions:

$$C|_{t=0} = C_0, \tag{3.2}$$

$$\frac{\partial C}{\partial\theta} = 0 \quad \text{at} \quad \theta = 0 \quad \text{and} \quad \theta_0, \tag{3.3}$$

$$C \quad \text{is finite at} \quad r = 0, \tag{3.4}$$

$$C|_{\phi} = C|_{\phi+2\pi} \qquad (n=3). \tag{3.5}$$

(In the two-dimensional case, we have for simplicity by symmetry confined ourselves in the above to the half-region $0 \leqslant \theta \leqslant \theta_0$.) The first of these conditions represents a prescribed initial solute concentration, with $C_0(r, \theta, (\phi))$ a specified function. The second represents the condition of symmetry about the cone axis, together with the requirement of no flux through the duct walls. The remaining conditions (3.4) and (3.5) respectively represent the requirements of boundedness of the concentration field and single-valuedness of the latter in the azimuthal angle ϕ.

As the velocity field and molecular diffusion coefficient are both independent of the angle ϕ, this angle constitutes a 'dead' degree of freedom over which one can integrate in the $n = 3$ case. (Of course, in the $n = 2$ case no such integration is required.) To ultimately establish the macrotransport equation (see (5.1)), we therefore need solve only for the azimuthally averaged concentration field:

$$c(r, \theta, t) \overset{\text{def}}{=} \int_0^{2\pi} C(r, \theta, \phi, t) \mathrm{d}\phi \qquad (n = 3). \tag{3.6}$$

Upon introduction of the dimensionless quantities

$$\tau = \frac{tD}{\theta_0^2 r_0^2}, \qquad \Theta = \frac{\theta}{\theta_0}, \qquad R = \frac{r}{r_0}, \tag{3.7a,b,c}$$

where r_0 is a characteristic radial distance, (3.1)–(3.5) become

$$\frac{\partial c}{\partial \tau} + \varepsilon \frac{q(\Theta)}{R^{n-1}} \frac{\partial c}{\partial R} - \kappa \varepsilon^2 \frac{1}{R^{n-1}} \frac{\partial}{\partial R}\left(R^{n-1} \frac{\partial c}{\partial R}\right) - \frac{1}{R^2 \sin^{n-2}(\Theta\theta_0)} \frac{\partial}{\partial \Theta}\left(\sin^{n-2}(\Theta\theta_0) \frac{\partial c}{\partial \Theta}\right) = 0, \tag{3.8}$$

$$c|_{\tau=0} = c_0, \tag{3.9}$$

$$\frac{\partial c}{\partial \Theta} \quad \text{at} \quad \Theta = 0 \quad \text{and} \quad 1, \tag{3.10}$$

$$c \quad \text{is finite at} \quad R = 0, \tag{3.11}$$

in which c_0 is the prescribed value of c at $\tau = 0$,

$$q(\Theta) = \frac{Q(\Theta\theta_0)}{\overline{Q}}, \tag{3.12}$$

$$\varepsilon = \frac{\theta_0^2 \overline{Q}}{r_0^{n-2} D} \tag{3.13}$$

and

$$\kappa = \left(\frac{D r_0^{n-2}}{\overline{Q}\theta_0}\right)^2. \tag{3.14}$$

In the above, $\overline{Q} \equiv \int Q(\theta)\mathrm{d}S / \int \mathrm{d}S$ is the algebraically signed average 'volumetric' flow rate, explicitly defined as

$$\overline{Q} = \int_0^{\theta_0} Q(\theta) \sin^{n-2}\theta \mathrm{d}\theta \Big/ \int_0^{\theta_0} \sin^{n-2}\theta \mathrm{d}\theta. \tag{3.15}$$

The dimensionless parameter $|\varepsilon|$ is proportional to the ratio of the angular diffusion

time τ_D to the convection time τ_Q from $r = 0$ to r_0, respectively defined as

$$\tau_D = \frac{\theta_0^2 r_0^2}{D}, \qquad \tau_Q = \frac{r_0^n}{n|\bar{Q}|}. \tag{3.16a,b}$$

4. Multiple-timescale analysis

Equation (3.8) may be recast in terms of the comparable Green's function (Brenner & Edwards 1993), the latter being formally equivalent to the conditional probability density $P(R, \Theta, \tau | R', \Theta')$ that a unit tracer introduced into the system at position (R', Θ') at time $\tau = 0$ is present at the position (R, θ) at time τ:

$$\frac{\partial P}{\partial \tau} + \varepsilon \frac{q(\Theta)}{R^{n-1}} \frac{\partial P}{\partial R} - \kappa \varepsilon^2 \frac{1}{R^{n-1}} \frac{\partial}{\partial R}\left(R^{n-1} \frac{\partial P}{\partial R}\right) - \frac{1}{R^2 \sin^{n-2}(\Theta\theta_0)} \frac{\partial}{\partial \Theta}\left(\sin^{n-2}(\Theta\theta_0) \frac{\partial P}{\partial \Theta}\right) = \frac{\delta(R - R')}{R^{n-1}} \frac{\delta(\Theta - \Theta')}{\sin^{n-2}(\Theta\theta_0)} \delta(\tau). \tag{4.1}$$

This equation is to be solved subject to the boundary conditions

$$\frac{\partial P}{\partial \Theta} = 0 \quad \text{at} \quad \Theta = 0 \quad \text{and} \quad 1, \tag{4.2}$$

$$P \quad \text{is finite at} \quad R = 0, \tag{4.3}$$

$$R^{n-1} P \to 0 \quad \text{as} \quad R \to \infty. \tag{4.4}$$

In the long-time limit and for $|\varepsilon| \ll 1$, the above system of microscale equations may be reduced to a comparable macroscale equation for the cross-sectionally averaged probability density, defined as

$$\overline{P} = \int_0^1 P \sin^{n-2}(\Theta\theta_0) \mathrm{d}\Theta \Big/ \int_0^1 \sin^{n-2}(\Theta\theta_0) \mathrm{d}\Theta, \tag{4.5}$$

through the use of a multiple-timescale analysis in which ε is a small parameter. (The physical implications of the requirement that ε be small are discussed in §6.) To accomplish this macrotransport analysis, introduce into (4.1) the sequence of time variables

$$\tau_m = \varepsilon^m \tau \qquad (m = 0, 1, 2, ..., \infty), \tag{4.6}$$

each of which is to be treated as an independent variable, and write

$$P(R, \Theta, \tau | R', \Theta') \equiv P(R, \Theta, \tau_0, \tau_1, \tau_2, ... | R', \Theta'). \tag{4.7}$$

Expand P in a perturbation series in ε:

$$P = \sum_{n=0}^{\infty} \varepsilon^n P_n(R, \Theta, \tau_0, \tau_1, \tau_2, ... | R', \Theta'). \tag{4.8}$$

The time derivative appearing on the left-hand side of (4.1) may then be written as

$$\frac{\partial P}{\partial \tau} = \sum_{n=0}^{\infty} \sum_{m=0}^{\infty} \varepsilon^{n+m} \frac{\partial P_n}{\partial \tau_m}. \tag{4.9}$$

Substitute (4.8) and (4.9) into (4.1) and equate terms of equal order in ε to obtain the

following recursive sequence of equations governing the respective P_n:

$$\frac{\partial P_0}{\partial \tau_0} - \frac{1}{R^2 \sin^{n-2}(\Theta\theta_0)} \frac{\partial}{\partial \Theta}\left(\sin^{n-2}(\Theta\theta_0)\frac{\partial P_0}{\partial \Theta}\right) = \frac{\delta(R-R')}{R^{n-1}} \frac{\delta(\Theta-\Theta')}{\sin^{n-2}(\Theta\theta_0)}\delta(\tau), \quad (4.10)$$

$$\frac{\partial P_1}{\partial \tau_0} + \frac{\partial P_0}{\partial \tau_1} + \frac{q(\Theta)}{R^{n-1}}\frac{\partial P_0}{\partial R} - \frac{1}{R^2 \sin^{n-2}(\Theta\theta_0)} \frac{\partial}{\partial \Theta}\left(\sin^{n-2}(\Theta\theta_0)\frac{\partial P_1}{\partial \Theta}\right) = 0 \quad (4.11)$$

and

$$\frac{\partial P_2}{\partial \tau_0} + \frac{\partial P_1}{\partial \tau_1} + \frac{\partial P_0}{\partial \tau_2} + \frac{q(\Theta)}{R^{n-1}}\frac{\partial P_1}{\partial R} - \frac{1}{R^2 \sin^{n-2}(\Theta\theta_0)} \frac{\partial}{\partial \Theta}\left(\sin^{n-2}(\Theta\theta_0)\frac{\partial P_2}{\partial \Theta}\right)$$
$$-\frac{\kappa}{R^{n-1}}\frac{\partial}{\partial R}\left(R^{n-1}\frac{\partial P_0}{\partial R}\right) = 0, \quad (4.12)$$

up to and including terms of second order in ε. Each such equation is to be solved subject to the same boundary conditions set forth for P in (4.2)–(4.4).

Multiply (4.10) by $\sin^{n-2}(\Theta\theta_0)$, integrate from $\Theta = 0$ to $\Theta = 1$ and apply the boundary condition (4.2) to obtain

$$\frac{\partial \overline{P}_0}{\partial \tau_0} = 0 \qquad (\tau_0 > 0). \quad (4.13)$$

Thus, for long times ($\tau_0 \gg 1$),

$$P_0 \sim \overline{P}_0(R, \tau_1, \tau_2, \ldots | R') + \text{exp}, \quad (4.14)$$

in which 'exp' denotes terms which decay exponentially in τ_0.

Substitution of (4.14) into (4.11) furnishes an asymptotic equation governing P_1 for long times. Multiply (4.11) by $\sin^{n-2}(\Theta\theta_0)$, integrate from $\Theta = 0$ to 1, and apply the boundary condition (4.2) to derive the asymptotic relation

$$\frac{\partial \overline{P}_1}{\partial \tau_0} + \frac{\partial \overline{P}_0}{\partial \tau_1} + \frac{1}{R^{n-1}}\frac{\partial \overline{P}_0}{\partial R} \sim \text{exp}. \quad (4.15)$$

The second and third terms in the above equation are independent of τ_0. Thus, in order to prevent secular growth of $\overline{P}_1$ in τ_0, it is required that

$$\frac{\partial \overline{P}_0}{\partial \tau_1} = -\frac{1}{R^{n-1}}\frac{\partial \overline{P}_0}{\partial R}, \quad (4.16)$$

whence

$$\overline{P}_1 \sim \text{exp}. \quad (4.17)$$

(This secular growth argument is equivalent to that used by Chatwin (1970).) Substitute (4.14), (4.16), and (4.17) into (4.11) to obtain

$$\frac{1}{\sin^{n-2}(\Theta\theta_0)}\frac{\partial}{\partial \Theta}\left(\sin^{n-2}(\Theta\theta_0)\frac{\partial P_1}{\partial \Theta}\right) \sim R^{3-n}\frac{\partial \overline{P}_0}{\partial R}(q(\Theta) - 1) + \text{exp}. \quad (4.18)$$

The above may be solved subject to the boundary and normalization conditions (4.2) and (4.17), yielding

$$P_1 \sim f(\Theta)R^{3-n}\frac{\partial \overline{P}_0}{\partial R} + \text{exp}, \quad (4.19)$$

where the function $f(\Theta)$ represents the solution of the boundary value problem

$$\frac{1}{\sin^{n-2}(\Theta\theta_0)}\frac{\partial}{\partial\Theta}\left(\sin^{n-2}(\Theta\theta_0)\frac{\partial f}{\partial\Theta}\right) = q(\Theta) - 1, \tag{4.20}$$

subject to the conditions

$$\frac{\partial f}{\partial\Theta} \quad \text{at} \quad \Theta = 0 \quad \text{and} \quad 1, \tag{4.21}$$

$$\int_0^1 f(\Theta)\sin^{n-2}(\Theta\theta_0)\mathrm{d}\Theta = 0. \tag{4.22}$$

It remains only to find the terms of $O(\varepsilon^2)$. By substituting the respective solutions (4.14) and (4.19) for P_0 and P_1 into (4.12) and integrating over the cross-sectional area, the dependence of $\overline{P}_0$ upon τ_2 may be obtained:

$$\frac{\partial\overline{P}_2}{\partial\tau_0} + \frac{\partial\overline{P}_0}{\partial\tau_2} - \frac{\kappa}{R^{n-1}}\frac{\partial}{\partial R}\left(R^{n-1}\frac{\partial\overline{P}_0}{\partial R}\right) - \frac{F(\theta_0)}{R^{n-1}}\frac{\partial}{\partial R}\left(R^{3-n}\frac{\partial\overline{P}_0}{\partial R}\right) \sim \exp. \tag{4.23}$$

Here,

$$-F(\theta_0) = \int_0^1 f(\Theta)q(\Theta)\sin^{n-2}(\Theta\theta_0)\mathrm{d}\Theta \Big/ \int_0^1 \sin^{n-2}(\Theta\theta_0)\mathrm{d}\Theta, \tag{4.24}$$

or in an alternative form which may be derived through use of (4.20)–(4.22) in the above,

$$F(\theta_0) = \int_0^1 \left(\frac{\mathrm{d}f}{\mathrm{d}\Theta}\right)^2 \sin^{n-2}(\Theta\theta_0)\mathrm{d}\Theta \Big/ \int_0^1 \sin^{n-2}(\Theta\theta_0)\mathrm{d}\Theta. \tag{4.25}$$

Prevention of the secular growth of $\overline{P}_2$ in τ_0 requires that

$$\frac{\partial\overline{P}_0}{\partial\tau_2} - \frac{\kappa}{R^{n-1}}\frac{\partial}{\partial R}\left(R^{n-1}\frac{\partial\overline{P}_0}{\partial R}\right) - \frac{F(\theta_0)}{R^{n-1}}\frac{\partial}{\partial R}\left(R^{3-n}\frac{\partial\overline{P}_0}{\partial R}\right) \sim 0 \tag{4.26}$$

and

$$\overline{P}_2 \sim \exp. \tag{4.27}$$

5. The macrotransport equation

The macrotransport equation governing $\overline{P}$ (accurate to $O(\varepsilon^2)$) may be found by integrating (4.9) over the cross-sectional area and substituting (4.14), (4.16), (4.17), (4.26), and (4.27) into the resulting expression to obtain (in dimensional form)

$$\frac{\partial\overline{P}}{\partial t} + \frac{\overline{Q}}{r^{n-1}}\frac{\partial\overline{P}}{\partial r} - \frac{D}{r^{n-1}}\frac{\partial}{\partial r}\left(r^{n-1}\frac{\partial\overline{P}}{\partial r}\right) - \frac{\overline{D}_c}{r^{n-1}}\frac{\partial}{\partial r}\left(r^{3-n}\frac{\partial\overline{P}}{\partial r}\right) = \frac{\delta(r-r')}{r^{n-1}}\frac{\delta(t)}{\displaystyle\int_0^{\theta_0}\sin^{n-2}\theta\mathrm{d}\theta}, \tag{5.1}$$

wherein

$$\overline{D}_c = \frac{\overline{Q}^2}{D}\theta_0^2 F(\theta) \tag{5.2}$$

represents the convective contribution to the dispersivity. This equation is valid for both positive (diverging flow) and negative (converging flow) values of $\overline{Q}$. Note that inasmuch as $F(\theta_0)$ is always non-negative (see (4.25)) it follows that $\overline{D}_c$ is always non-negative irrespective of the direction of flow.

6. Range of validity of the global equation

The present analysis is valid provided that $|\varepsilon| \ll 1$ and $\tau_0 \gg 1$ (or equivalently $t \gg \theta_0^2 r_0^2/D$). It can be shown that the first requirement is automatically satisfied provided that the second constraint is met. A tracer particle initially introduced into a diverging or converging flow at the radial position r' will (on average) be located at time t at the point

$$r_t = [n\bar{Q}t + (r')^n]^{(1/n)}. \tag{6.1}$$

(For converging flows, for which $\bar{Q} < 0$, the above is valid for $t < (r')^n/n|\bar{Q}|$, after which time the solute particle will, on average, have flowed out of the cone through the apex along with the solvent.) Substitution into (6.1) of the inequality

$$t \gg \frac{\theta_0^2 r_0^2}{D} \tag{6.2}$$

followed by subsequent rearrangement gives

$$\frac{n\theta_0^2 \bar{Q} r_0^2}{D[r_t^n - (r')^n]} \ll 1. \tag{6.3}$$

The characteristic length r_0 is to be chosen as the larger of the two lengths r_t and r'. Thus, for diverging flows ($Q > 0$) $r_0 = r_t$, while for converging flows ($Q < 0$) $r_0 = r'$. After replacement of r_0 in (3.13) and (6.3) with the appropriate length, comparison of the two constraints reveals that the requirement (6.2) is more restrictive than the requirement $|\varepsilon| \ll 1$. Thus, satisfaction of a single constraint suffices to guarantee that the macrotransport description (5.1) of the process is applicable.

Observe that ε, the ratio of the transverse diffusion time to the convection time, scales as r_0^{-n+2} (3.13). Hence, in three dimensions a macrotransport description of the process is always possible for some sufficiently large r_0 or, equivalently, for long enough times. For the two-dimensional case, the situation is different. In this case, ε is independent of r_0. Thus, circumstances exist for which no macrotransport description is possible, regardless of the lengthscale of the channel. Physically, this means that in some instances the transverse diffusion time τ_D is greater than or equal to the convection time τ_Q. In such cases, corresponding to large flow rates or apex angles, a particle introduced into a diverging flow will be swept downstream so quickly that insufficient time exists for it to sample all angular positions. This is so because as the particle is convected downstream, the transverse distance through which it must travel in order to reach the most distant streamlines increases more rapidly than $(Dt)^{1/2}$, the lateral distance through which it has diffused. It may appear that this limitation would not be present for the case of converging flow, for which the particle encounters a decreasing cross-sectional area as it is convected toward the apex of the system. This impression is erroneous, however, for although the particle is confronted with a smaller area to sample, its velocity increases at precisely the same rate at which the cross-sectional area decreases, so that the particle still has insufficient time in which to sample all of the streamlines. In such circumstances, a purely asymptotic description of the process cannot be valid since the particle will 'remember' the angular position θ' at which it was originally introduced.

In contrast, in three dimensions, a macrotransport description is always possible for some sufficiently large r_0. Although the transverse distance that a particle in a diverging flow must sample increases as it is convected through the cone, the velocity with which it is convected decreases rapidly enough that the particle can sample all of the streamlines if given enough time. Likewise, in converging flow, the

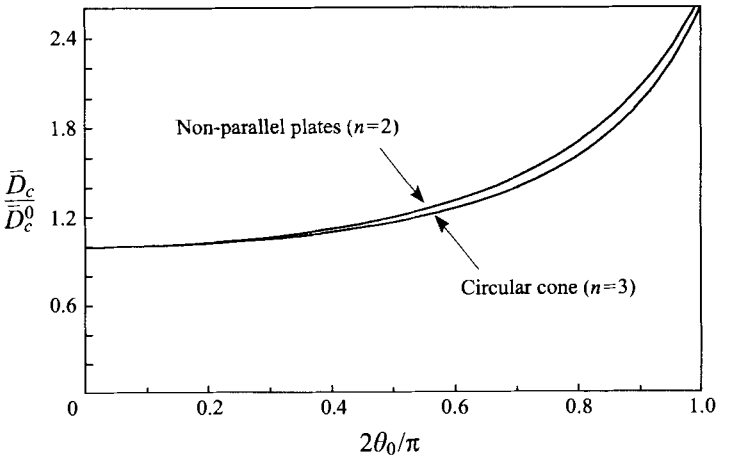

FIGURE 2. Convective contribution, $\bar{D}_c$, to the dispersion coefficient for axisymmetric low-Reynolds-number flow between non-parallel plates or in a circular cone. Observe that for the limiting case where $\theta_0 = \pi/2$, the dispersivity ratio quantified by the ordinate attains the limiting values of $105/4\pi^2$ ($n = 2$) and $128/5\pi^2$ ($n = 3$).

velocity increases more slowly than the cross-sectional area decreases, thus enabling the particle to sample all of the streamlines.

7. Examples: low-Reynolds-number flow

7.1. *Non-parallel plates*

Application of (4.20)–(4.22) together with (4.25) and (5.2) to the case of creeping flow between non-parallel plates, for which the velocity is given by (2.5), gives

$$\bar{D}_c = \frac{\bar{Q}^2}{D}\frac{1}{12}\frac{6\theta_0^2 - 6\sin^2 2\theta_0 + 9\theta_0 \sin 2\theta_0 \cos 2\theta_0 + 4\theta_0^2 \sin^2 2\theta_0}{(\sin 2\theta_0 - 2\theta_0 \cos 2\theta_0)^2}. \tag{7.1}$$

It may be shown in the limit $\theta_0 \to 0$ that this reduces to the classical result for Taylor dispersion between flat plates. To do so, replace the flow rate with the average velocity, $\bar{V} \overset{\text{def}}{=} \bar{Q}/r$, introduce the half-distance, $h \overset{\text{def}}{=} \theta_0 r$, between the plates, and expand in a Taylor series about $\theta_0 = 0$ to obtain

$$\bar{D}_c \sim \bar{D}_c^0 \left(1 + \frac{4}{15}\theta_0^2 + \ldots\right), \tag{7.2}$$

where

$$\bar{D}_c^0 = \frac{2}{105}\frac{\bar{V}^2 h^2}{D} \qquad (n = 2) \tag{7.3}$$

is the classical result (Wooding 1960) for flow between parallel plates.

A plot of the convective contribution (7.1) to the dispersivity versus the half-angle between the flat plates is given in figure 2. The dispersivity increases appreciably with increasing angles owing to the fact that the transverse velocity gradients $\partial v_r/\partial\theta$ increase with increasing angles of divergence.

For this two-dimensional situation, the macrotransport equation governing the

angularly averaged conditional probability density $\overline{P}(r,t|r')$ is

$$\frac{\partial \overline{P}}{\partial t} + \frac{\overline{Q}}{r}\frac{\partial \overline{P}}{\partial r} - \frac{\overline{D}^*}{r}\frac{\partial}{\partial r}\left(r\frac{\partial \overline{P}}{\partial r}\right) = \frac{\delta(r-r')}{r}\delta(t), \tag{7.4}$$

in which

$$\overline{D}^* = D + \overline{D}_c \tag{7.5}$$

is the total Taylor–Aris dispersivity. The solution of (7.4) may be found through use of Laplace transforms to be

$$\overline{P} = \frac{1}{2\overline{D}^* t}\left(\frac{r}{r'}\right)^{Pe^*/2} \exp\left(-\frac{[r^2+(r')^2]}{4\overline{D}^* t}\right) \mathrm{I}_{|Pe^*|/2}\left(\frac{rr'}{2\overline{D}^* t}\right), \tag{7.6}$$

in which

$$Pe^* = \frac{\overline{Q}}{\overline{D}^*} \tag{7.7}$$

is the effective Péclet number and I_v is the modified Bessel function of order v .

Note that the two-dimensional case is unique in that the macrotransport equation (5.1) assumes the same functional form as the symmetric, purely radial form of the microscale equation (4.1). In contrast the three-dimensional macroscale equation possesses a different structure than the original microscale equation in regard to the final term appearing on the left-hand side of (5.1).

7.2. *Circular cone*

Solution of (4.20)–(4.22) for low-Reynolds-number flow in a circular cone, for which the velocity is given by (2.6), followed by subsequent use of (4.25) and (5.2) yields (see figure 2):

$$\overline{D}_c = \frac{\overline{Q}^2}{15D}\frac{(1-\zeta_0)(2-3\zeta_0-23\zeta_0^2-38\zeta_0^3-8\zeta_0^4-2)+30\zeta_0^2(1+\zeta_0)^2\ln[2(\zeta_0+1)^{-1}]}{(1+2\zeta_0)^2(1-\zeta_0)^3}, \tag{7.8}$$

in which $\zeta_0 = \cos\theta_0$. As in the two-dimensional case, replacement of the flow rate with the average velocity $\overline{V} \overset{\text{def}}{=} \overline{Q}/r^2$, introduction of the 'radius' $h \overset{\text{def}}{=} \theta_0 r$ at any point in the cone, and expansion of the above in a Taylor series about $\theta_0 = 0$ demonstrates that in the limit $\theta_0 \to 0$, the dispersion coefficient reduces to the classical result for Taylor dispersion in a circular cylinder (Taylor 1953; Aris 1956):

$$\overline{D}_c \sim \overline{D}_c^0\left(1+\frac{13}{60}\theta_0^2+\ldots\right), \tag{7.9}$$

where

$$\overline{D}_c^0 = \frac{1}{48}\frac{\overline{V}^2 h^2}{D} \qquad (n=3). \tag{7.10}$$

The macroscale equation in three dimensions is

$$\frac{\partial \overline{P}}{\partial t} + \frac{\overline{Q}}{r^2}\frac{\partial \overline{P}}{\partial r} - \frac{\overline{D}}{r^2}\frac{\partial}{\partial r}\left(r^2\frac{\partial \overline{P}}{\partial r}\right) - \frac{\overline{D}_c}{r^2}\frac{\partial^2 \overline{P}}{\partial r^2} = \frac{\delta(r-r')}{r^2}\frac{\delta(t)}{1-\cos\theta_0}. \tag{7.11}$$

In this case, in contrast with the two-dimensional case (7.4), the convective dispersivity $\overline{D}_c$ contributes to the net transport differently than does the molecular diffusivity D, as can be seen by comparing the final two terms on the left-hand side of the above.

8. Discussion

8.1. *Solute conservation*

Although our analysis is valid for both converging and diverging flows, the semi-infinite configuration of the conical domain, coupled with the singularity of the velocity field at the apex $r = 0$, leads to fundamental differences in the temporal behaviour of the probability densities for the respective cases of $Q > 0$ and $Q < 0$, all other things being equal. In particular, the total probability of a solute particle being located within the cone is conserved for diverging flow, but not for converging flow; rather, in the latter case there is a continuous loss of solute through the apex. Mathematically, this behaviour may be seen by integrating the microscale equation (4.1) over the infinite domain V_∞ of the cone and applying the boundary conditions (4.2)–(4.4) to obtain (in dimensional form)

$$\frac{\mathrm{d}}{\mathrm{d}t}\int_{V_\infty} P\,\mathrm{d}V = Q\overline{P}|_{r=0}, \tag{8.1}$$

where $\mathrm{d}V \equiv \mathrm{d}S\mathrm{d}r \equiv r^{n-1}\sin^{n-2}\theta\mathrm{d}r\mathrm{d}\theta(\mathrm{d}\phi)$ is a 'volume' element. For $Q = 0$, the total amount of solute initially present in the cone is conserved for all time, as in the known results (Carslaw & Jaeger 1959) for pure diffusion in a wedge and in a circular cone. However, examination of the solution (7.6) of the macrotransport equation for $n = 2$ reveals that for $Q > 0$, $\overline{P}|_{r=0} = 0$ for all times $t > 0$. Hence, for diverging flow, the particle is always contained within the cone. The explanation for this phenomenon lies in the functional form of the velocity field, which varies inversely with radial position. A solute particle is never able to diffuse backwards to the apex of the cone because its diffusion is opposed by an infinite velocity in the positive direction. In contrast, for $Q < 0$, $\overline{P}$ assumes a finite positive value at the origin, namely

$$\overline{P}|_{r=0} = r'(2\overline{D}^* t)^{-(|Pe^*|/2+1)}\exp\left(-\frac{(r')^2}{4\overline{D}^* t}\right). \tag{8.2}$$

Thus, solute exits the cone at its apex, eventually becoming entirely depleted.

8.2. *Asymptotic behaviour of the microscale field*

Not only does our analysis result in an asymptotic equation for the macroscale probability density $\overline{P}$, but concomitantly it also furnishes an asymptotic approximation to the exact microscale probability density P. In particular, in combination, (4.8), (4.14) and (4.19) yield

$$P(r,\theta,t|r',\theta') \sim \overline{P}(r,t|r') + \frac{\overline{Q}\theta_0^2}{D} f(\theta/\theta_0) r^{3-n}\frac{\partial \overline{P}}{\partial r} + \ldots\ . \tag{8.3}$$

This asymptotic expression is similar in appearance to the first two terms occurring in the expansion of Taylor (1954) (subsequently expanded by Gill 1967), with the exception of the presence of the coefficient r^{3-n} occurring in the second term on the right-hand side of the above, which arises from the varying cross-sectional area of the duct.

8.3. *Dispersion in curvilinear, cross-sectionally varying channels and ducts*

The methods described herein may be utilized to analyse dispersion in generally varying channels and ducts whose boundaries are curvilinear rather than rectilinear. We use general orthogonal curvilinear coordinates (Happel & Brenner 1983) (q_1, q_2, q_3) and consider 'unidirectional' flows whose streamlines lie along the q_1 coordinate

curves. Flow through a hyperbolic cone or 'Venturi' tube (Happel & Brenner 1983, p. 150) as in figure 3 constitutes an example of this class. We will confine ourselves to the three-dimensional, duct-flow case, although the analysis is easily extended to two-dimensional, channel flows. The surface of the duct will be taken to be defined by the functional relation $F(q_2, q_3) = \text{const}$. The continuity equation in such a coordinate system is

$$\frac{\partial}{\partial q_1}\left(\frac{u_1}{h_2 h_3}\right) = 0, \tag{8.4}$$

in which the scalar $u_1(q_1, q_2, q_3)$ is the speed $h_i(q_1, q_2, q_3)$ and is the metrical coefficient in the q_i direction. The velocity field is thus of the form

$$u_1 = h_2 h_3 q(q_2, q_3). \tag{8.5}$$

In this notation, the convection–diffusion equation governing the conditional probability density $P(q_1, q_2, q_3, t|q_1', q_2', q_3')$ is

$$\frac{\partial P}{\partial t} + h_1 h_2 h_3 q(q_2, q_3)\frac{\partial P}{\partial q_1} - D h_1 h_2 h_3 \left[\frac{\partial}{\partial q_1}\left(\frac{h_1}{h_2 h_3}\frac{\partial P}{\partial q_1}\right) + \frac{\partial}{\partial q_2}\left(\frac{h_2}{h_1 h_3}\frac{\partial P}{\partial q_2}\right) + \frac{\partial}{\partial q_3}\left(\frac{h_3}{h_1 h_2}\frac{\partial P}{\partial q_3}\right)\right] = \delta(t)\delta(q_1 - q_1')\delta(q_2 - q_2')\delta(q_3 - q_3')h_1 h_2 h_3. \tag{8.6}$$

We now follow a procedure similar to that used in our previous analysis. It is again required that the convection time be much larger than the transverse diffusion time. The ratio of these times is given by $|\varepsilon|$, where

$$\varepsilon = \frac{\overline{Q}\|q_2\|^2\|h_1\|\,\|h_3\|}{D\|q_1\|\,\|h_2\|}. \tag{8.7}$$

Here, the brackets $\|...\|$ denote an appropriate norm of the quantity they bound; q_2 is the coordinate corresponding to the largest of the two transverse directions, and the constant $\overline{Q}$ is related to the volumetric flow rate Q through the duct (both $\overline{Q}$ and Q being independent of the 'axial' distance q_1) as follows:

$$\overline{Q} = Q \Big/ \int_{S_1} \mathrm{d}q_2 \mathrm{d}q_3, \tag{8.8}$$

where

$$Q = \int_{S_1} q(q_2, q_3)\mathrm{d}q_2 \mathrm{d}q_3. \tag{8.9}$$

Here, S_1 denotes the 'cross-sectional' domain corresponding to the surface defined by $q_1 = \text{const.}$ and bounded by the curvilinear duct wall, $F(q_2, q_3) = \text{const}$.

Upon performing a multiple-timescale analysis similar to that for the circular cone, the macrotransport equation governing the macroscale conditional probability density $\overline{P}(q_1, t|q_1')$ is ultimately found to be

$$\frac{\partial \overline{P}}{\partial t} + \frac{Q}{\overline{A}}\frac{\partial \overline{P}}{\partial q_1} - \frac{D}{\overline{A}}\frac{\partial}{\partial q_1}\left(\chi\frac{\partial \overline{P}}{\partial q_1}\right) - \frac{1}{\overline{A}}\frac{\partial}{\partial q_1}\left(\overline{D}_c\frac{\partial \overline{P}}{\partial q_1}\right) = \frac{1}{\overline{A}}\delta(t)\delta(q_1 - q_1'), \tag{8.10}$$

in which

$$\overline{A}(q_1) = \int_{S_1} \frac{\mathrm{d}A_1}{h_1} \tag{8.11}$$

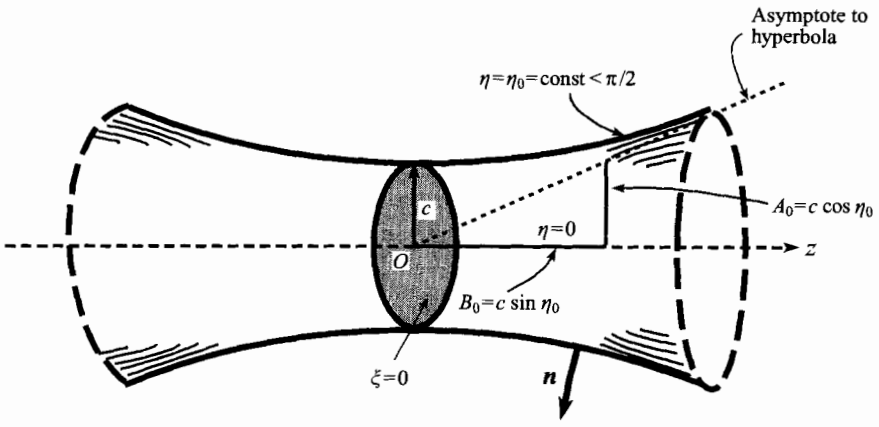

FIGURE 3. Hyperboloid of revolution ('Venturi' tube). The coordinate system is $q_1 = \xi$, $q_2 = \eta$, $q_3 = \phi$, with S_1 the domain $0 \leqslant \eta \leqslant \eta_0$, $0 \leqslant \phi < 2\pi$. The duct throat, corresponding to the value $\xi = 0$, is of radius c. The duct centreline corresponds to the value $\eta = 0$ and the unit normal vector $\boldsymbol{n}$ to the duct surface η_0 is the unit vector $\boldsymbol{i}_\eta$ in oblate spherical coordinates. The major and minor axes A_0 and B_0 of the hyperboloid η_0 are respectively as shown in the sketch, with $B_0/A_0 = \tan\eta_0$; thus, the angle between the z-axis and the dashed asymptote corresponds physically to the angle η_0.

and

$$\chi(q_1) = \int_{S_1} h_1 \mathrm{d}A_1, \tag{8.12}$$

where $\mathrm{d}A_1 = \mathrm{d}q_2\mathrm{d}q_3/h_2h_3$ is a differential areal element on the surface $q_1 = \text{const}$. The convective contribution $\overline{D}_c$ to the dispersion required in (8.10) is given by

$$\overline{D}_c(q_1) = -\frac{\overline{Q}^2}{D}\int_{S_1} v(q_2, q_3)g(q_1, q_2, q_3)\mathrm{d}q_2\mathrm{d}q_3, \tag{8.13}$$

with

$$v = \frac{q(q_2, q_3)}{\overline{Q}}. \tag{8.14}$$

The function $g(q_1, q_2, q_3)$ appearing above represents the solution of the following boundary value problem:

$$\left[\frac{\partial}{\partial q_2}\left(\frac{h_2}{h_1h_3}\frac{\partial g}{\partial q_2}\right) + \frac{\partial}{\partial q_3}\left(\frac{h_3}{h_1h_2}\frac{\partial g}{\partial q_3}\right)\right] = v - \frac{\overline{A}^{-1}}{h_1h_2h_3}\int_{S_1}\mathrm{d}q_2\mathrm{d}q_3, \tag{8.15}$$

$$\boldsymbol{n}\cdot\nabla g = 0 \quad \text{on} \quad F(q_2, q_3) = \text{const.}, \tag{8.16}$$

$$\int_{S_1} g\frac{\mathrm{d}A_1}{h_1} = 0. \tag{8.17}$$

In the above, $\boldsymbol{n}$ represents the unit vector normal to the surface of the duct. Use of (8.15)–(8.17) in (8.13) allows $\overline{D}_c$ to be written in an alternative form which demonstrates that the dispersivity is non-negative:

$$\overline{D}_c = \int_{S_1}\left[\left(h_2\frac{\partial g}{\partial q_2}\right)^2 + \left(h_3\frac{\partial g}{\partial q_3}\right)^2\right]\frac{\mathrm{d}A_1}{h_1}. \tag{8.18}$$

The 'average' probability density function appearing in the macrotransport equation

(8.10) is defined as

$$\overline{P} \overset{\text{def}}{=} \int_{S_1} P \frac{\mathrm{d}A_1}{h_1} \Big/ \int_{S_1} \frac{\mathrm{d}A_1}{h_1}. \tag{8.19}$$

In our prior discussion of dispersion in a cone and between non-parallel plates, the average utilized was an *area* average. The above average is equal to the *volume* average taken over an infinitesimal volume centred at a given 'axial' position q_1

$$\overline{P} = \lim_{\delta \to 0} \left(\int_{S_1} \int_{q_1-\delta}^{q_1+\delta} P \mathrm{d}V \Big/ \int_{S_1} \int_{q_1-\delta}^{q_1+\delta} \mathrm{d}V \right), \tag{8.20}$$

where $\mathrm{d}V = \mathrm{d}q_1 \mathrm{d}q_2 \mathrm{d}q_3 / h_1 h_2 h_3$ is a differential volume element. The quantity defined in (8.20) is identically equal to the area average in the conical geometry considered previously, since in that case h_1 is independent of q_2 and q_3.

The *physical* form of (8.10) becomes especially transparent in circumstances where the metrical coefficient h_1 is, at most, a function only of q_1, and hence independent of q_2 and q_3. Since the quantity $\mathrm{d}q_1/h_1 = \mathrm{d}l_1$, say, is the arc length, measured along the q_1-coordinate curve (Happel & Brenner 1983), it follows that when h_1 is of the form $h(q_1) \equiv h_1(l_1)$, the quantity $\mathrm{d}l_1$ is then an exact differential. Consequently, the arc length l_1 possesses a global physical interpretation. In such circumstances, (8.11) and (8.12) become $\overline{A} = A_1/h_1$ and $\chi = h_1 A_1$, where $A_1(q_1) \equiv A_1(l_1)$ is the 'cross-sectional' area of the duct corresponding to the domain S_1. Moreover, the 'volume average' probability density $\overline{P}$ defined by (8.19) becomes identical with the (curvilinear) area-average probability density $\int_{S_1} P \mathrm{d}A_1/A_1$. In these circumstances, the macrotransport equation (8.10) governing $\overline{P} \equiv \overline{P}(l_1, t | l_1')$ adopts the form

$$\frac{\partial \overline{P}}{\partial t} + \frac{Q}{A_1} \frac{\partial \overline{P}}{\partial l_1} - \frac{D}{A_1} \frac{\partial}{\partial l_1} \left(A_1 \frac{\partial \overline{P}}{\partial l_1} \right) - \frac{1}{A_1} \frac{\partial}{\partial l_1} \left(\overline{D}_c^* \frac{\partial \overline{P}}{\partial l_1} \right) = \frac{1}{A_1} \delta(t) \delta(l_1 - l_1'), \tag{8.21}$$

in which

$$\overline{D}_c^* = \overline{D}_c h_1. \tag{8.22}$$

An example of a configuration for which h_1 is independent of q_2 and q_3 occurs for the circular cone case, where (Happel & Brenner 1983, p. 504) with the choice $(q_1, q_2, q_3) = (r, \theta, \phi)$, we have that

$$h_1 = 1, \qquad h_2 = 1/r, \qquad h_3 = 1/r \sin\theta, \tag{8.23}$$

and hence $l_1 = r$, $A_1 = \chi = 2\pi(1 - \cos\theta_0) r^2$. In this case (8.21) reproduces (7.11).

8.3.1. *Dispersion in a flared, 'Venturi' tube*

As an application of the general curvilinear analysis embodied in (8.10), consider the problem of convection and diffusion in a 'Venturi' tube (i.e. a hyperboloid of revolution of one sheet, as in figure 3). Such a flow may be described in oblate spheroidal coordinates ($-\infty < \xi < \infty$, $0 \leqslant \eta \leqslant \pi/2$, $0 \leqslant \phi \leqslant 2\pi$), in which the hyperboloidal surface of the tube is $\eta = \eta_0$. (This coordinate system is identical to that appearing in Happel & Brenner (1983, p. 512) with the exception of the ranges of η and ξ.) These coordinates are related to circular cylindrical coordinates (z, R, ϕ), having their origin O at the centre of the tube throat, by the relations

$$z = c \sinh\xi \cos\eta, \qquad R = c \cosh\xi \sin\eta. \tag{8.24a,b}$$

The coordinate surfaces $\xi = \text{const.}$ and $\phi = \text{const.}$ are respectively oblate spheroids and meridian planes, the latter containing the z-axis.

The axisymmetric stream function for the low-Reynolds-number flow through the tube is (Happel & Brenner 1983; Sampson 1891)

$$\Psi = \frac{Q}{2\pi}\frac{\zeta(\zeta^2 - 3\zeta_0^2) - (1 - 3\zeta_0^2)}{(1 + 2\zeta_0)(1 - \zeta_0)^2}, \tag{8.25}$$

in which $\zeta = \cos\eta$ and $\zeta_0 = \cos\eta_0$ denotes the surface of the duct, so that the streamlines are hyperbolas, lying on the coordinate surfaces $\eta = $ const. in a meridian plane ($\phi = $ const). In contrast to the previous cases of flow in a circular cone or between non-parallel plates, in the present geometry the flow contains both 'diverging' and 'converging' regions and no singularity exists at the origin.

In this oblate spheroidal coordinate system, the quantities necessary for determination of the macroscale equation are

$$h_1 = h_2 = \frac{1}{c(\cosh^2\xi - \sin^2\eta)^{1/2}}, \tag{8.26}$$

$$h_3 = \frac{1}{c\cosh\xi\sin\eta} \tag{8.27}$$

and

$$q(\eta) = -\frac{\mathrm{d}\Psi}{\mathrm{d}\eta}. \tag{8.28}$$

The condition which must be met in order for the present multiple-timescale analysis to apply is again $|\varepsilon| \ll 1$, with

$$\varepsilon = \frac{\overline{Q}\eta_0^2}{Dc\xi_0\cosh\xi_0}, \tag{8.29}$$

in which ξ_0 is a characteristic value† of the 'axial' coordinate ξ, and

$$\overline{Q} = \frac{Q}{2\pi\eta_0}. \tag{8.30}$$

Solution of (8.15) subject to (8.16) and (8.17) yields

$$\frac{\partial g(\eta,\xi)}{\partial\eta} = \frac{3\eta_0}{c\cosh\xi\sin\eta}\frac{(1-\zeta)(\zeta-\zeta_0)(\zeta+\zeta_0+1)(\cosh^2\xi+\zeta_0^2-1)}{(1+2\zeta_0)(1-\zeta_0)^2(3\cosh^2\xi+\zeta_0^2+\zeta_0-2)}. \tag{8.31}$$

The resulting macroscale equation is then of the form (8.10) with

$$\overline{A}(\xi) = c^3C_0\lambda(3\lambda^2 + C_1), \tag{8.32}$$

$$\chi(\xi) = 3cC_0\lambda, \tag{8.33}$$

$$\overline{D}_c(\xi) = \frac{\overline{Q}^2}{cD}\frac{(\lambda^2 + C_2)^2}{\lambda(3\lambda^2 + C_1)^2}C_3, \tag{8.34}$$

in which $\lambda = \cosh\xi$, and the constants C_i are functions only of η_0 as follows:

$$C_0 = (\tfrac{2}{3})\pi(1 - \zeta_0), \tag{8.35}$$

$$C_1 = \zeta_0^2 + \zeta_0 - 2, \tag{8.36}$$

† For long axial distances from the tube throat, the distance $r = (R^2 + z^2)^{1/2}$ from the origin approximates $r \approx c\cosh\xi$, while the transverse distance approximates $h \approx c\eta_0\cosh\xi$. The parameter ε is thus proportional to the ratio of the transverse diffusion time τ_D to the axial convection time τ_Q, respectively defined as $\tau_D = h^2/D$, $\tau_Q = r^3/\overline{Q}$.

$$C_2 = \zeta_0^2 - 1, \tag{8.37}$$

$$C_3 = \frac{6\pi\eta_0^2}{5} \frac{(1-\zeta_0)(2-3\zeta_0-23\zeta_0^2-28\zeta_0^3-8\zeta_0^4)+30\zeta_0^2(\zeta_0+1)^2\ln[2(\zeta_0+1)^{-1}]}{(1+2\zeta_0)^2(1-\zeta_0)^4}. \tag{8.38}$$

The above Venturi tube results may be compared with the circular cone results, (7.8)–(7.11), as follows. Referring to figure 3, it is seen that at large distances $|\xi| \to \infty$ along the axis, the hyperboloidal duct surface is isomorphic with the surface of the circular cone of half-angle $\theta_0 \equiv \eta_0$ in figure 1(*b*). From (8.24*a*, *b*), we find that the distance $r = (R^2+z^2)^{\frac{1}{2}}$ from the origin O is $r = c(\cosh^2\xi - cos^2\eta)^{\frac{1}{2}}$, which for $|\xi| \to \infty$ asymptotes to $r \sim c\cosh\xi$. Additionally, from (8.26), we see that, asymptotically $h_1 \sim (c\cosh\xi)^{-1}$, which is independent of η and ϕ, and thus asymptotically fulfils the requirement set forth in the paragraph following (8.20). Use of the above asymptotic relation for h_1 and the dispersivity (8.34) in (8.22) reveals that in this limit, $\overline{D}_c^*$ is independent of the axial position $l_1 \sim r$ (l_1 being calculated from its definition, $\mathrm{d}l_1 = \mathrm{d}\xi/h_1$), and may therefore be brought to the outside of the derivative in which it appears in the macrotransport equation (8.21). The ratio $\overline{D}_c^*/A_1$ then reduces to the form

$$\frac{\overline{D}_c^*}{A_1} = \frac{\overline{Q}^2}{D} \frac{C_3}{18\pi(1-\zeta_0)r^2}, \tag{8.39}$$

which may be shown, through use of the respective (albeit slightly different) definitions (8.27) and (3.15) for $\overline{Q}$ in the hyperboloidal and conical cases, to be exactly equal to the dispersivity (7.8) in the case of a circular cone, bearing in mind that $\theta_0 \equiv \eta_0$. Straightforward calculation shows that the other terms appearing in the macrotransport equation (8.21) are also identical to their counterparts in the circular cone case, (7.11).

Finally, we note that the case of flow through a circular aperture in a wall occurs when $\eta_0 = \pi/2$ ($\zeta_0 = 0$).

This work was supported by a National Science Foundation Graduate Fellowship to M.D.B. and by the Office of Basic Energy Sciences of the Department of Energy.

REFERENCES

ACKERBERG, R. C. 1965 The viscous incompressible flow inside a cone. *J. Fluid Mech.* **21**, 47–81.

ARIS, R. 1956 On the dispersion of a solute in a fluid flowing through a tube. *Proc. R. Soc. Lond.* A **235**, 66–77.

BRENNER, H. & EDWARDS, D. A. 1993 *Macrotransport Processes.* Butterworth-Heinemann.

CARSLAW, H. S. & JAEGER, J. C. 1959 *Conduction of Heat in Solids.* Oxford University Press.

CHATWIN, P. C. 1970 The approach to normality of the concentration distribution of a solute in a solvent flowing along a straight pipe. *J. Fluid Mech.* **20**, 321–352.

FRANKEL, I. & BRENNER, H. 1991 Generalized Taylor dispersion phenomena in unbounded shear flows. *J. Fluid Mech.* **230**, 147–181.

GILL, W. N. 1967 Analysis of axial dispersion with time variable flow. *Chem. Engng Sci.* **22**, 1013–1017.

GILL, W. N. & GÜCERI, U. 1971 Laminar dispersion in Jeffrey-Hamel flows: Part 1. Diverging channels. *AIChE J.* **17**, 207–214.

GOLDSTEIN, S. 1965*a* *Modern Developments in Fluid Dynamics*, vol. 1. Dover (reprint).

GOLDSTEIN, S. 1965*b* On backward boundary layers and flow in converging passages. *J. Fluid Mech.* **21**, 33–45.

HAPPEL, J. & BRENNER, H. 1983 *Low Reynolds Number Hydrodynamics.* Kluwer.

MERCER, G. N. & ROBERTS, A. J. 1990 Centre manifold description of contaminant dispersion in channels with varying flow properties. *SIAM J. Appl. Maths* **50**, 1547–1565.

PAGITSAS, M., NADIM, A. & BRENNER, H. 1986 Multiple time scale analysis of macrotransport processes. *Physica* **135**A, 533–550.

ROUSE, H. 1959 *Advanced Mechanics of Fluids*. Wiley.

SAMPSON, R. A. 1891 On Stoke's current function. *Phil. Trans. R. Soc. Lond.* A **182**. 449–518.

SMITH, R. 1983 Longitudinal dispersion coefficients for varying channels. *J. Fluid Mech.* **130**, 299–314.

TAYLOR, G. I. 1921 Diffusion by continuous movements. *Proc. Lond. Math. Soc.* **21**, 196–212.

TAYLOR, G. I. 1953 Dispersion of soluble matter in a solvent flowing slowly through a tube. *Proc. R. Soc. Lond.* A **219**, 186–203.

TAYLOR, G. I. 1954 Conditions under which dispersion of a solute in a stream of solvent can be used to measure molecular diffusion. *Proc. R. Soc. Lond.* A **225**, 473–477.

WOODING, R. A. 1960 Instability of a viscous fluid of variable density in a vertical Hele-Shaw cell. *J. Fluid Mech.* **7**, 501–515.